JCTC Journal of Chemical Theory and Computation

Article

pubs.acs.org/JCTC

How Does Darunavir Prevent HIV-1 Protease Dimerization?

Danzhi Huang* and Amedeo Caflisch*

Department of Biochemistry, University of Zürich, Winterthurerstrasse 190 CH-8057 Zürich, Switzerland

Supporting Information

ABSTRACT: The drug Darunavir (DRV) is a potent inhibitor of HIV-1 protease (PR), a homodimeric essential enzyme of the AIDS virus. Recent experimental data suggest that DRV is able to prevent dimerization of HIV-1 PR, which, together with its high affinity for the mature enzyme, has been linked to the high genetic barrier to the development of viral resistance. The mechanism of dimerization inhibition and the binding mode(s) of DRV to monomeric HIV-1 PR are unknown. Here, multiple molecular dynamics simulations with explicit solvent (for a total of 11 μs with the CHARMM force field and 1 μs with the Amber force field) show that the monomer of HIV-1 PR is structurally stable and reveal a major binding mode of DRV. This binding mode is stabilized by favorable interactions between the apolar groups of DRV and the hydrophobic residues Ile32, Ile47, Ile50, Ile54, Pro79, Val82, and Ile84. The binding mode to monomeric HIV-1 PR identified by molecular dynamics is different from the two binding modes observed in the crystal structure of the complex with dimeric HIV-1 PR. As an example, there are no interactions between DRV and the catalytic Asp25 in the binding mode to monomeric HIV-1 PR revelead by the simulations. In contrast, the simulations show extensive and stable interactions between DRV and the flap (residues 46−55), which are likely to sterically hinder the formation of the flap interface as observed in the dimeric structure. Which of the two mechanisms of inhibition (dimerization inhibition by association with the flap or binding to the active site of the mature enzyme) dominates might depend on the HIV-1 PR mutations, and it is likely that dimerization inhibition is predominant for multiple mutations at the active site in multidrug resistant strains.

1. INTRODUCTION

Acquired immunodeficiency syndrome (AIDS) is caused by the human immunodeficiency virus (HIV), which encodes, among other indispensable enzymes, an aspartic protease (HIV-1 PR) whose proteolytic activity is essential for viral replication.[1] There are 10 inhibitors of HIV-1 PR used routinely in the clinics to fight AIDS.[2] A major problem with most of these, as well as others that have failed in clinical trials, is that rapid mutation of HIV can lead to drug resistance.[3,4] Darunavir (abbreviated here as DRV, Figure 1), the inhibitor of HIV-1 PR most recently approved by the FDA,[5] has shown to be less susceptible to viral resistance than the previously approved HIV-1 PR inhibitors.[6,7] It has been suggested that the superior profile of resistance of DRV is due, at least in part, to its inhibition of the dimerization of HIV-1 PR,[8,9] which is a homodimer in its native functional state. Yet, the mechanism of inhibition of HIV-1 PR dimerization by DRV is not known.

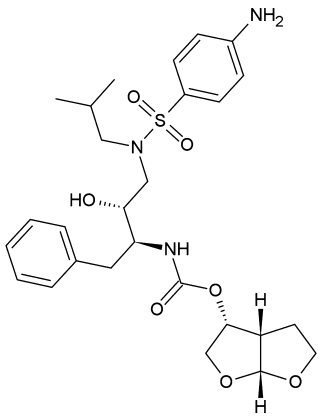

Figure 1. Chemical structure of Darunavir (abbreviated as DRV in the text).

There is indirect evidence from experimental and computational studies that HIV-1 PR has a structurally stable monomeric fold despite it assuming a homodimeric state in the mature form under physiological conditions. In other words, monomer folding and dimerization of HIV-1 PR are decoupled, as suggested by molecular dynamics (MD) simulations.[10−13] Experimentally, nuclear magnetic resonance (NMR) spectroscopy studies of mutants that destabilize the interface have suggested that HIV-1 PR has a (meta)stable monomeric form.[14−16] Recently, it has been shown by NMR and size-exclusion chromatography that the protease of HIV-2, another retrovirus which can cause AIDS, can assume a stable monomeric structure.[17] Other retroviral proteases, e.g., from spumaretroviruses, have been reported to exist mainly in the monomeric form.[18]

The available experimental data suggest that DRV has more than one binding mode in HIV-1 PR. The X-ray structures of two HIV-1 PR mutants show that DRV binds at the active site and at an exosite on the surface of one of the two flaps (PDB files 2HS1 and 2HS2).[19] The latter binding mode is likely to be an artifact of the crystallization conditions for the following reasons. First, DRV is surrounded by four HIV-1 PR molecules, and most of the interactions and contacting surface of DRV involve three symmetry-related neighboring HIV-1 PRs. In particular, the bis-tetrahydrofuran moiety of DRV, which was designed to optimize potency,[20] is not in contact with the flap.

Received: January 18, 2012
Published: April 12, 2012

Table 1. Details of MD Simulations of Monomeric HIV-1 PR

name	HIV-1 PR monomer mutant	no. of DRV molecules	initial binding mode	no. of trajectories	length of individual trajectories (ns)	total simulation time (ns)
Apo1	V32I/L33I			3	100	300
Apo2	V32I/L33F/I54M/V82A			3	100	300
Apo3	V32I/L33F/I54M/V82I			3	100	300
Apo4	V32I/L33F/I54M/I84 V			3	100	300
Rand1	V32I/L33I	2	random[a]	98	15−25	1800
Rand2	V32I/L33F/I54M/V82I	2	random[a]	87	20−30	2500
X1	V32I/L33I	1	X-ray1[b]	20	60	1200
X2	V32I/L33I	1	X-ray2[b]	20	60	1200
Xflap	V32I/L33I	1	X-ray (flap)[c]	20	20	400
MD1	V32I/L33I	1	MD1[d]	5	500	2500
MD1-A[e]	V32I/L33I	1	MD1[d]	2	500	1000

[a]The initial distance between any atom of HIV-1 PR and DRV was larger than 6 Å. [b]There are two possible orientations of DRV in monomeric HIV-1 PR because the active site of HIV-1 PR is at the dimer interface.[19] [c]Binding mode on the solvent-exposed surface of the flap observed by X-ray crystallography.[19] [d]Most populated binding mode observed in the 40 X1 and X2 runs. [e]These two control simulations were carried out using the Amber force field.

Second, given that the homodimeric structure has an intrinsic symmetry, it is not clear why the exosite is only on one of the two flaps and not in both. Third, the exosite binding mode does not appear in the X-ray structures of 27 HIV-1 PR (mutants) cocrystallized with DRV (PDB codes in the Supporting Information). Also, there is no supporting evidence by NMR spectroscopy, and only one binding site for DRV to HIV-1 PR has been deduced from a surface plasmon resonance study.[21] On the other hand, another kinetic analysis has shown mixed-type competitive−uncompetitive inhibition of HIV-1 PR by DRV (and the chemically related amprenavir).[22]

Here, we use explicit solvent MD simulations to analyze the structural stability of monomeric HIV-1 PR and search for binding modes of DRV. This simulation study was motivated by the following questions: Is HIV-1 PR structurally stable as a monomer? Does DRV bind to monomeric HIV-1 PR? If there is a major binding mode of DRV, does it explain the mechanism of dimerization inhibition? Are the (meta-)stable binding modes of DRV consistent with its superior resistance profile? The simulation results provide evidence that monomeric HIV-1 PR has a well-defined structure except for strong disorder at both terminal segments. Importantly, the MD simulations and clustering analysis reveal a major binding mode of DRV to monomeric HIV-1 PR which is significantly different from those observed in the crystal structure of the complex with mature HIV-1 PR. This binding mode is stable during the 0.5 μs time scale of the MD runs and is stabilized mainly by hydrophobic interactions with residues in the substrate binding site.

2. METHODS

MD Simulations. The coordinates of the V32I/L33I mutant of HIV-1 PR in complex with DRV were downloaded from the protein database (PDB code 2HS1). This X-ray structure was chosen because of its ultrahigh resolution of 0.84 Å.[19] Note that V32I/L33I is a drug-resistant mutation which does not influence the binding affinity or antiviral activity of DRV. To reproduce neutral pH conditions, the side chains of aspartates and glutamates were negatively charged, those of lysines and arginines were positively charged, and the His69 side chain was neutral and protonated at the N_ε atom. The structure of monomeric HIV-1 PR was prepared at neutral pH as the experimental results of highest relevance for the present simulation study were obtained under physiological conditions.[8] It has been reported that the equilibrium dissociation constant of dimeric HIV-1 PR at pH 5.5, which is the optimal pH value for catalytic activity, is about 17 times lower than at pH 7.[23] Note that the pH value of 5.5 would have required a different protonation state only for His69 (positively charged instead of neutral) with marginal influence on the main simulation results because the His69 side chain has a distance of about 25 Å and 20 Å from the tip of the flap and the carboxy groups of the two catalytic aspartates, respectively.

The structure of monomer A from the PDB file 2HS1 was immersed in a triclinic box of pre-equilibrated water molecules. The size of the box was chosen to have a minimal distance of 13 Å between the boundary and any atom of the protein. Water molecules within 2.4 Å of any heavy atom of the protein or DRV were removed except for six water molecules present in the crystal structure. The simulation system contained 21 sodium and 24 chloride ions to approximate an ionic strength of about 150 mM and to compensate for the total charge of the HIV-1 PR monomer, which is +3 electron units. The MD simulations were carried out with Gromacs 4.5.3[24,25] using the CHARMM PARAM22 force field[26] and the TIP3P model of water.[27] The parameters of DRV were determined according to the general CHARMM force field.[28] To check whether the results are dependent on the choice of force field, two 0.5-μs runs of the complex of DRV with monomeric HIV-1 PR were carried out with the Amber force field[29] and the previously reported Amber parameters for DRV.[30]

Periodic boundary conditions were applied, and electrostatic interactions were evaluated using the particle-mesh Ewald summation method.[31] The van der Waals interactions were truncated at a cutoff of 10 Å, and a switch function was applied starting at 8 Å. The temperature of 310 K was kept constant with an external bath with velocity rescaling,[32] and the pressure was kept close to 1 atm using Berendsen et al.'s coupling algorithm.[33] The SHAKE algorithm was used to fix the covalent bonds involving hydrogen atoms. The integration time step was 2 fs, and snapshots were saved every 10 ps.

Multiple MD runs of monomeric HIV-1 PR were carried out for each of the three following systems: (1) apo, (2) in the presence of one molecule of DRV and starting from one of the three poses of DRV observed in the ultrahigh resolution crystal structure, and (3) in the presence of two DRV molecules

initially positioned at random in the bulk solvent. In the latter simulation system, the concentration of DRV is about 15 mM. Multiple MD runs with identical starting conformations were started with different initial random distributions of the atomic velocities. A list of all of the MD simulations of monomeric HIV-1 PR is given in Table 1.

To analyze the stability of the dimeric structure of the mutant V32I/L33F/I54M/V82I, two additional runs of 0.5 μs each were carried out. One of these two runs concerned the wild type sequence (and was started from the PDB structure 7UPJ upon removal of the inhibitor), while the other concerned the mutant V32I/L33F/I54M/V82I for which the mutated side chains were modified on the basis of the PDB structure 2HS1. The same simulation setup and protocols (with CHARMM PARAM22 force field) were used as for monomeric HIV-1 PR.

Cut-Based Free Energy Profile Analysis. The analysis of the MD trajectories was carried out with the programs CHARMM[34] and WORDOM.[35,36] The leader algorithm as implemented in WORDOM was employed for clustering according to the distance root-mean-square (DRMS) between two MD snapshots a and b, DRMS = $[n^{-1}\sum_{(i,j)}^{n}(d_{ij}^{a} - d_{ij}^{b})^2]^{1/2}$, which was calculated using the intermolecular distances d_{ij} between pairs of non-hydrogen atoms in DRV and the following 12 residues in the substrate binding site of HIV-1 PR: Asp25, Thr26, Gly27, Ala28, Asp29, Ile32, Ile47, Gly48, Gly49, Ile50, Val82, and Ile84. A DRMS threshold of 2 Å was used for clustering the 240 000 snapshots of the 2.4 μs sampling of the X1 and X2 runs.

The cut-based free energy profile method[37] was used to identify metastable states of DRV on the surface of monomeric HIV-1 PR and their relative stability. The input for the cut-based free energy profile calculation is the network of conformational transitions, which is derived from the direct transitions between clusterized snapshots (nodes of the network) sampled at a given time interval (10 ps here) along the MD simulations. For the calculation of the cuts and related free energy values, nodes are first sorted according to increasing mean first passage time to a reference node. After the sorting, nodes are partitioned into two groups A and B. Group A includes only the reference node at the beginning and is iteratively expanded by moving the kinetically closest node (i.e., the one with smallest mean first passage time) from group B to A. The cut is determined at every iteration, and the free energy is related to the maximum flow across the cut and approximated as $\Delta G = -kT \ln(Z_{AB})$, where Z_{AB} is the partition function of the cutting surface based on the mean first passage time (for further details, see Figure 2 of ref 38). The result is a one-dimensional profile along a reaction coordinate (the relative partition function) that preserves the barrier height between well-separated free energy basins.[37]

3. RESULTS AND DISCUSSIONS

Three types of MD simulations were carried out, and they are analyzed in the next three subsections. First, the stability of four mutants of monomeric HIV-1 PR was investigated by performing 12 runs of 0.1 μs each in the absence of DRV. Second, the binding modes of DRV to monomeric HIV-1 PR were explored by performing 185 and 3 × 20 MD runs started from completely dissociated DRV and its three poses derived from the crystal structure of dimeric HIV-1 PR. Finally, the most stable binding mode identified by MD was further validated by five MD runs of 0.5 μs each and two 0.5-μs runs with a different force field (Amber). The total simulation time is about 12 μs. Table 1 lists the simulated systems and other details including starting structure and length of individual simulations.

3.1. Stability and Flexibility of Monomeric HIV-1 PR. The structural stability of the HIV-1 PR monomer was studied previously using implicit solvent as well as short explicit water MD simulations.[10,11] Here, much longer explicit solvent MD simulations are carried out (12 runs of 0.1 μs each, Table 1) to assess the stability of four mutants of monomeric HIV-1 PR. One of them is the V32I/L33I mutant from the X-ray structure of the complex with DRV (PDB code 2HS1). Of the three remaining variants, the four-point mutants V32I/L33F/I54M/V82I and V32I/L33F/I54M/I84V cause DRV to lose dimerization inhibition, whereas V32I/L33F/I54M/V82A does not.[9] The Cα atomic fluctuations of the four mutants are similar (Figure 2), which suggests that differences in DRV

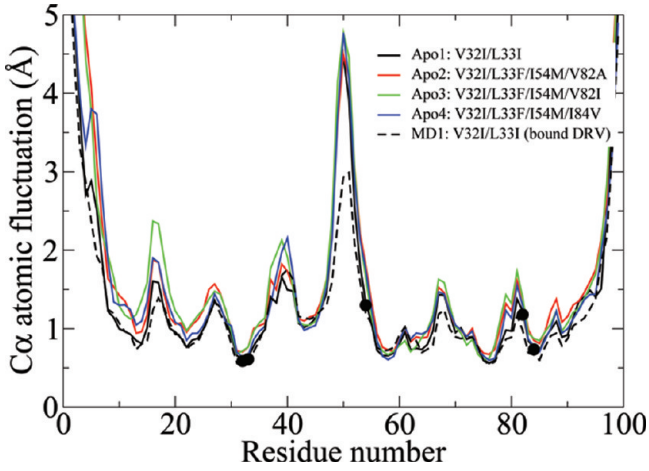

Figure 2. Flexibility of termini and flap of monomeric HIV-1 PR. The four mutants of monomeric HIV-1 PR have a similar profile of the C_α root-mean-square fluctuations along the 99-residue sequence (solid lines). In the presence of DRV (dashed line), the fluctuation profile does not change significantly except for the reduced mobility of the flap residues 46−55. Positions of point mutations are emphasized (black circles). Each line shows values of the fluctuations averaged over three runs of 100 ns each.

affinity for monomeric HIV-1 PR between V32I/L33F/I54M/V82I and V32I/L33F/I54M/V82A are due to the intermolecular interactions rather than differences in flexibility. The largest fluctuations are observed at the termini (residues 1−10 and 91−99) and the flap (residues 46−55). Excluding the flexible termini and the flap, the C_α root-mean-square deviation (RMSD) from the X-ray structure of HIV-1 PR (PDB code 2HS1) almost never exceeds 2 Å (Figure 3 and Figures S1 and S2). Interestingly, the time series of the RMSD from the crystal structure (Figure S3) indicates that the folded conformation of monomeric HIV-1 PR is preserved also with the Amber force field, which provides further evidence for the kinetic stability of the monomer. Congruent with the fluctuation and RMSD analysis, the average value and standard deviation of the radius of gyration are significantly smaller if one neglects the termini and the flap (10.8 ± 0.1 Å) than for the whole monomer (12.8 ± 0.3 Å, Figure S4). Fast changes of orientation of the flap are observed during the MD runs. As an example, the distance between the Cα atoms of Ile51 (at the flap tip) and Ile32 (at the base of the active site) oscillates between 12 and 22 Å on a

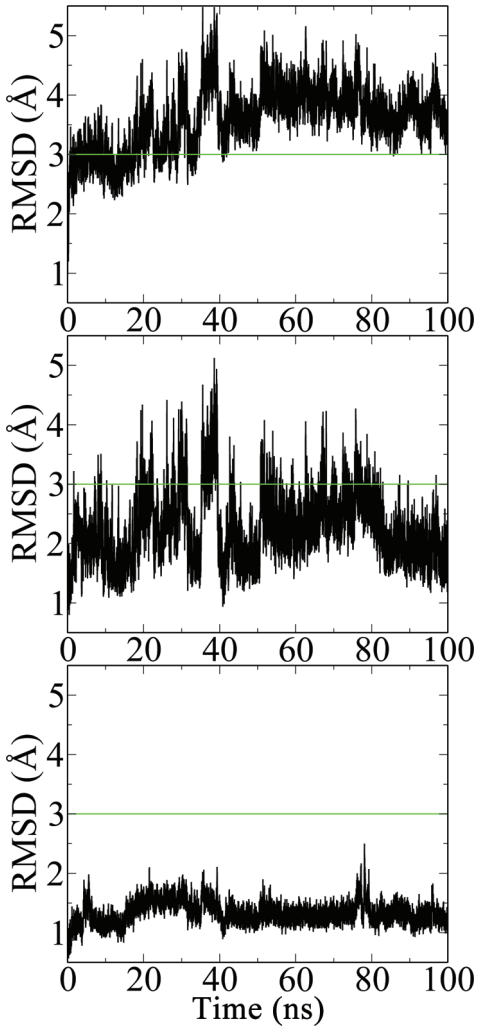

Figure 3. Structural stability of monomeric HIV-1 PR. Time series of the C_α RMSD from the X-ray structure of HIV-1 PR (PDB code 2HS1) during one of the three Apo1 runs. (Top) All 99 residues; (middle) without termini, i.e., considering only residues 11−90; (bottom) without termini and flap, i.e., considering only residues 11−45 and 56−90. The other 11 Apo1−4 runs show similar RMSD time series (Figures S1 and S2).

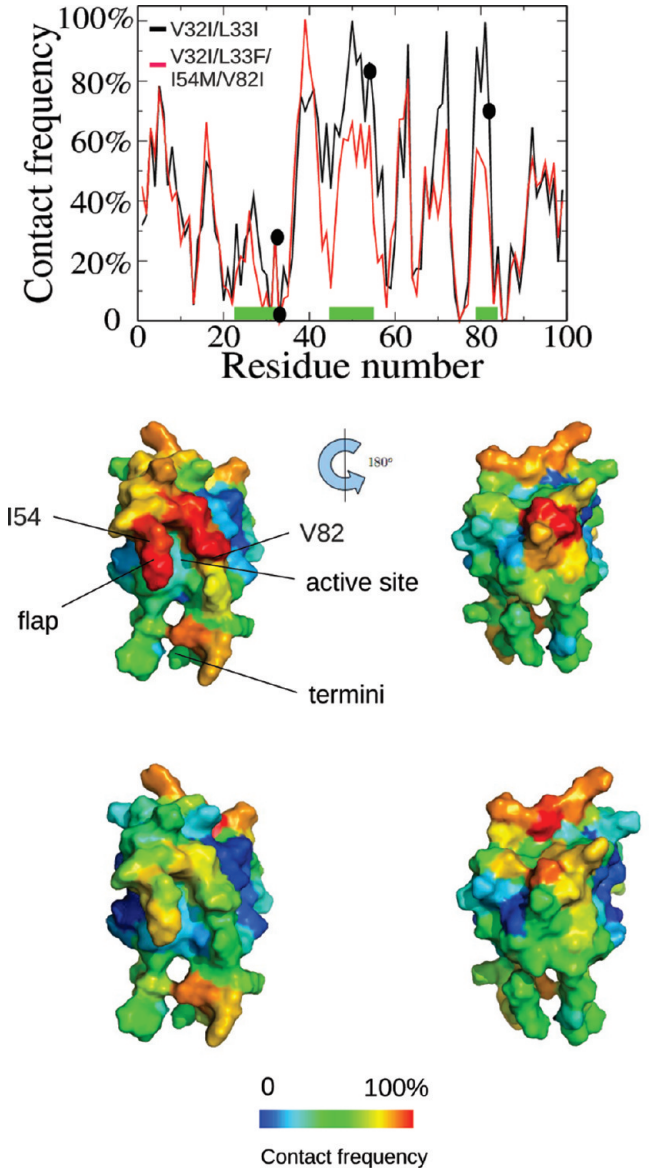

Figure 4. Map of DRV/HIV-1 PR monomer contact frequencies. (Top) Contact frequency as a function of HIV-1 PR residue number. The binding site residues and sites of mutations are emphasized by green rectangles and black circles, respectively. Note that the very high overlap for more than half of the residues indicates that the contact frequency has reached convergence, and the differences between the mutants V32I/L33I (black line) and V32I/L33F/I54M/V82I (red line), e.g., at the flap residues 46−55, are statistically significant. (Middle) Map of contact frequencies for the mutant V32I/L33I. (Bottom) Map of contact frequencies for the mutant V32I/L33F/I54M/V82I. The contact frequency is the percentage of MD snapshots in which the center of mass of any of the two DRV molecules is within 10 Å of any residue of monomeric HIV-1 PR. For V32I/L33I and V32I/L33F/I54M/V82I, 98 MD runs for a total of 1.8 μs and 87 MD runs for a total of 2.5 μs were used, respectively. All figures with structures were prepared by pyrol.[46]

5 to 50 ns time scale (Figure S5), which is consistent with NMR spectroscopy data for the monomeric R87K mutant[14] and dimeric HIV-1 PR.[39,40]

3.2. DRV Binding to Monomeric HIV-1 PR. To efficiently explore the association of DRV to monomeric HIV-1 PR, two sets of simulations were carried out. First, a total of 185 MD runs, of 15 to 30 ns each, were started from two DRV molecules initially positioned and oriented randomly with respect to monomeric HIV-1 PR in the simulation box (runs called Rand1 and Rand2 with mutants V32I/L33I and V32I/L33F/I54M/V82I, respectively, see Table 1). Only two DRV molecules (concentration of 15 mM) were used to avoid aggregation. Overall, DRV associates mainly to the flap and residues of the substrate binding site (Figure 4).

In the second set of simulations, 20 independent MD runs of 60 ns each were started from each of the two orientations of DRV in the active site as derived from the X-ray structure of the complex with mature HIV-1 PR.[19] Since DRV is not a symmetric molecule, two possible binding modes to the monomer exist, and both modes were used in the simulations (called X1 and X2, Table 1). Analysis of the 40 X1,2 runs reveals that multiple poses exist close to the residues of the substrate binding site. The cut-based free energy profile analysis[37] reveals two major free energy basins for DRV binding to monomeric HIV-1 PR (Figure 5). The barrier to unbinding from the most populated binding mode (called MD1) is about 3 kcal/mol. Remarkably, in eight of the 40 X1,2

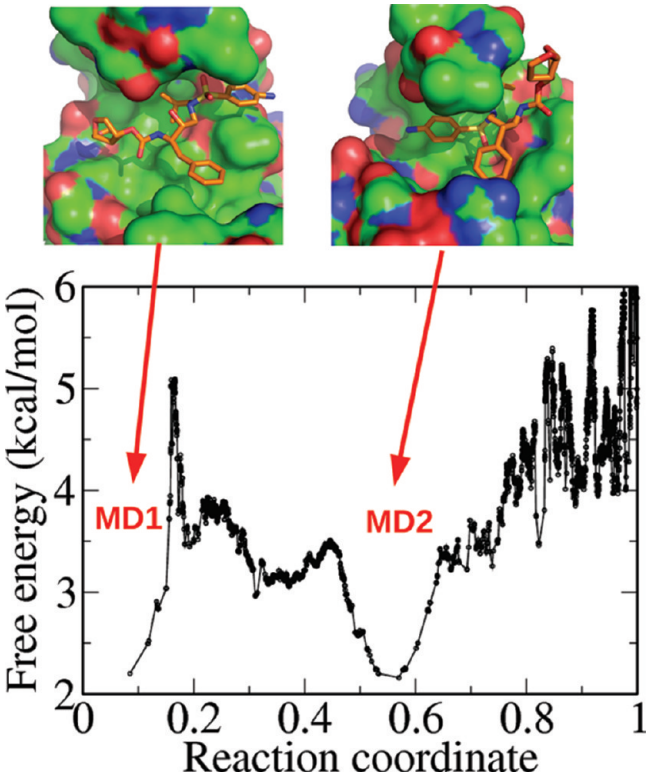

Figure 5. Binding modes of DRV into the HIV-1 PR monomer. (Top) The MD1 (left) and MD2 (right) poses of DRV (stick model, carbon atoms in orange) into monomeric HIV-1 PR (surface model with green, blue, and red patches corresponding to C, N, and O atoms, respectively). (Bottom) Cut-based free energy profile[37] of DRV binding. The most populated pose, i.e., most populated MD1 cluster, is used as a reference and the value of the reaction coordinate is zero for it. The 4500 data points correspond to the 4500 clusters obtained by DRMS clustering of the 240 000 snapshots of the X1 and X2 runs using a threshold of 2 Å.

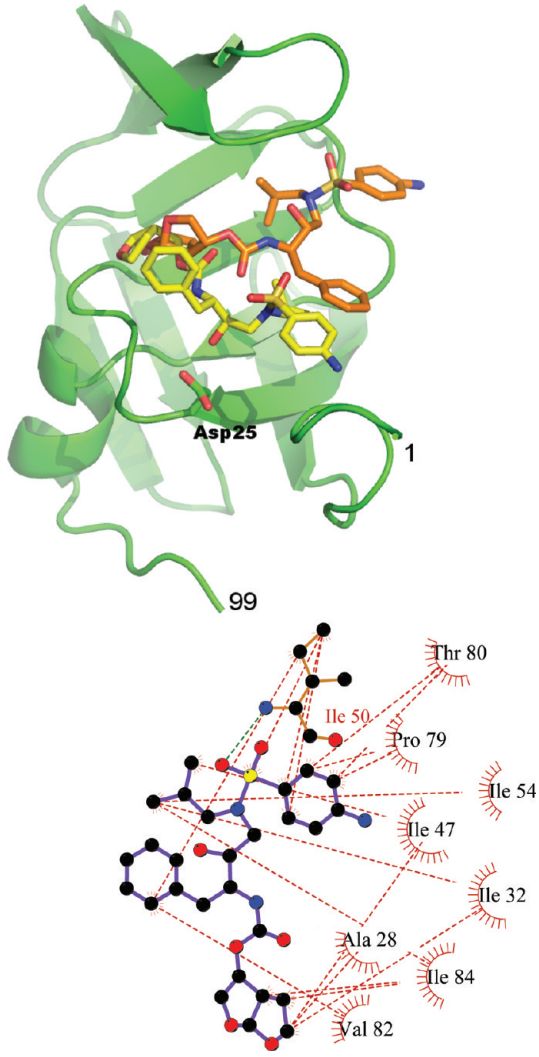

Figure 6. Comparison of binding mode of DRV to monomeric HIV-1 PR obtained by MD simulations (MD1) with the X-ray structure of the complex with dimeric HIV-1 PR. (Top) Overlap of DRV in the binding mode MD1 (stick model, carbon atoms in orange) to the X-ray structure of the complex with mature HIV-1 PR (carbon atoms in yellow). The two binding modes are superimposed using the Cα atoms of HIV-1 PR excluding the residues at the termini and flap which are flexible. The monomeric HIV-1 PR structure (snapshot from the MD runs) is rendered by green ribbons, while the X-ray structure of dimeric HIV-1 PR is not shown for clarity. (Bottom) Two-dimensional illustration of the MD1 binding mode. The red dashed lines are the most frequent hydrophobic contacts between DRV and individual residues of monomeric HIV-1 PR during the 2.5 μs of the elongated runs started from the MD1 binding mode. The program LIGPLOT was used to prepare this picture.[45]

simulations, DRV reaches spontaneously the MD1 binding mode (with DRMS < 2 Å, Figure S6), which is preserved until the end of the runs (see also subsection 3.3. Validation of Most Populated Binding Mode of DRV to Monomeric HIV-1 PR). A metastable binding mode (called MD2) is reached in 10 of the 40 X1,2 simulations, but in about five of them, it is not preserved until the end of the runs (Figure S6). The reduced stability of the MD2 pose is due, at least in part, to the orientation of the bis-tetrahydrofuran group which is exposed to solvent (Figure 5, top right). The comparison of MD1 with the binding mode in the X-ray structure of the homodimer (Figure 6) shows that DRV is not in contact with Asp25 (the residue of the catalytic dyad in mature homodimeric HIV-1 PR). The lack of direct interactions with Asp25 is consistent with the DRV inhibition of dimerization of the Asp25Ala mutant as measured by a cellular assay based on intermolecular FRET.[9] Another interesting feature of the MD1 binding mode is that the sulfonyl-(2-methylpropyl)amino moiety moves to the position originally occupied by the flap of the other monomer when in dimer format. As a consequence, the dimerization is likely to be hindered because the two flaps cannot associate (Figure 7). Another possible scenario is that the plasticity of the flap could allow for association with another monomer but with a significantly distorted active site and/or reduced stability of the dimeric state, and the presence of DRV would prevent substrate binding. In this context, it is important to note that the extensive interactions between Darunavir and the flap significantly reduce the flexibility of the latter as evidenced by smaller Cα atomic fluctuations (black dash line, Figure 2). The bis-tetrahydrofuran moiety binds at a similar position to that in the mature HIV-1 PR but with a different orientation. Its carbon atoms are involved in hydrophobic interactions with the Ile residues 32, 47, and 84 (Figure 6, bottom). However, since the substrate binding site is more solvent-exposed in the monomer than in the dimer, only one of the two hydrogen bonds involving the bis-tetrahydrofuran oxygens (and backbone NH groups of Asp29 and Asp30) is preserved but becomes a water-bridged hydrogen bond (Figure

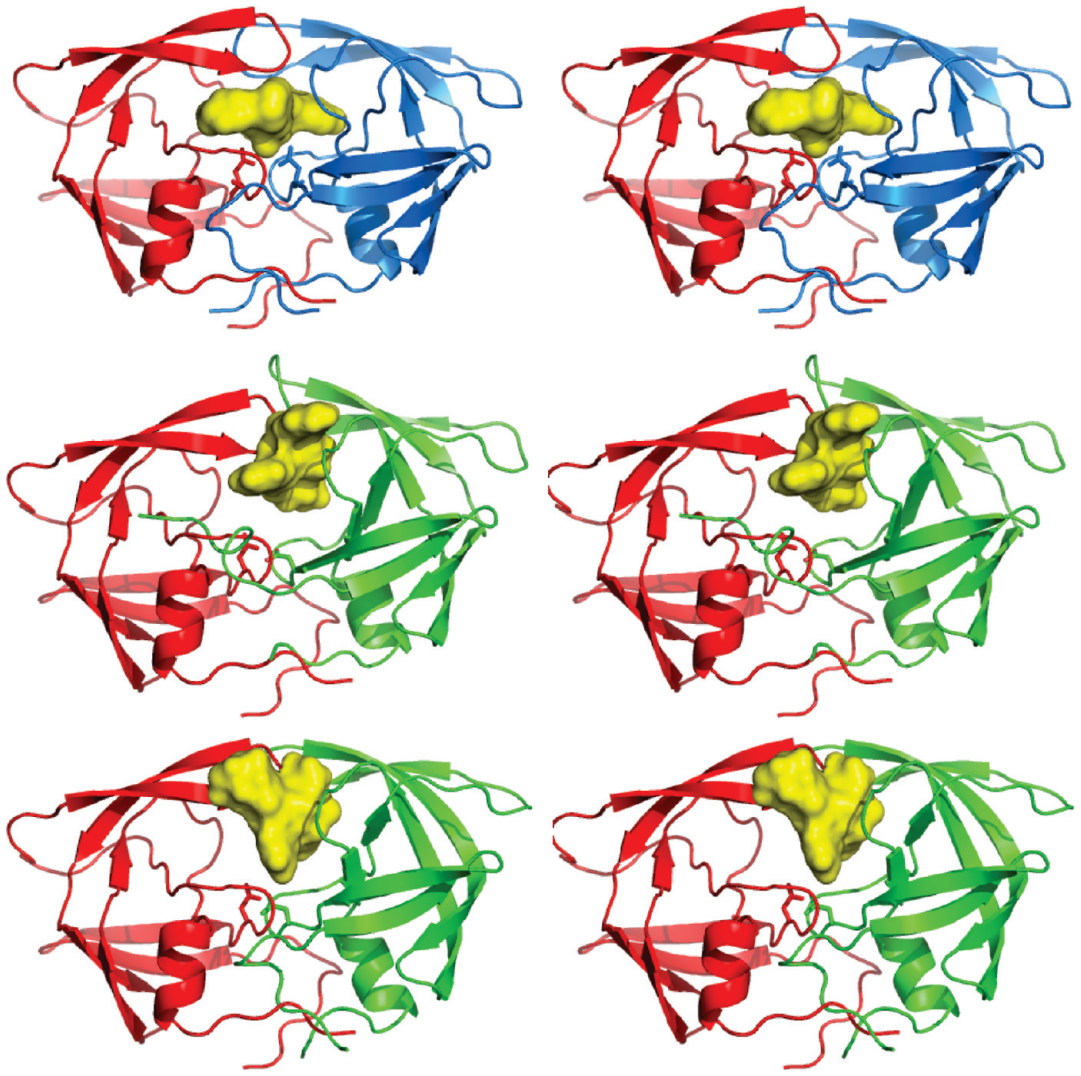

Figure 7. Binding of DRV to monomeric HIV-1 PR prevents dimerization. In these stereoviews DRV is shown by a yellow van der Waals surface, while the HIV-1 PR structure is rendered by a ribbon model with different colors for the two monomeric subunits. (Top) X-ray conformation of the complex between DRV and mature HIV-1 PR (PDB code 2HS1).[19] The bound DRV fits in the active site without affecting the flap interface. (Middle) DRV in the MD1 binding mode interferes with the dimerization of the flaps. The X-ray structure of dimeric HIV-1 PR (red, only one subunit is shown) is superimposed to monomeric HIV-1 PR (green) using the Cα atoms without the termini and flap. (Bottom) Same as middle for binding mode MD2.

S7). On the other hand, there is a direct hydrogen bond between one of the two sulfonamide oxygens and the backbone NH of Ile50 at the flap tip (Figure S8). Moreover, both phenyl rings of DRV are in van der Waals contact with the side chain of Ile50.

Finally, the binding mode at the exterior surface of the flap observed by X-ray crystallography[19] was assessed by 20 independent MD runs of 20 ns each. Notably, DRV unbinds from this site in 14 of the 20 runs (characteristic unbinding time of about 13 ns, Figure S9). This result is consistent with a kinetic binding study by surface plasmon resonance[21] and provides further evidence that the binding site at the flap surface is a crystal packing effect.[41]

3.3. Validation of Most Populated Binding Mode of DRV to Monomeric HIV-1 PR. The kinetic stability of the binding mode MD1 was further assessed by elongating five of the eight MD simulations that had spontaneously reached the MD1 binding mode. Strikingly, in all five runs, the MD1 binding mode is stable over the 0.5 μs time scale of the elongated trajectories with a DRMS almost always smaller than 2.0 Å (Figure 8 and Figure S10) except for a transient opening of the flap over about 30 ns in one of the five runs. Moreover, the interactions between DRV and the hydrophobic side chains in the substrate binding site of monomeric HIV-1 PR are preserved (Figure S11). The stability of the MD1 binding mode was also checked using the Amber force field.[42] Despite a slight shift and reorientation of the phenyl group, which results in a DRMS deviation of 2.2 Å from the MD1 pose obtained by the CHARMM force field, the main interactions of the MD1 binding mode are preserved. Furthermore, the time series of DRMS shows that the "Amber-refined" MD1 pose is stable over a time scale of 0.5 μs (Figure S12).

3.4. Analysis of a DRV-Resistant Mutant. The simulations with random initial positions and orientations of DRV with respect to monomeric HIV-1 PR were carried out with two mutants V32I/L33I and V32I/L33F/I54M/V82I. The V32I/L33F/I54M/V82I mutant forms mature (i.e., dimeric) HIV-1 PR even in the presence of a 1 μM concentration of

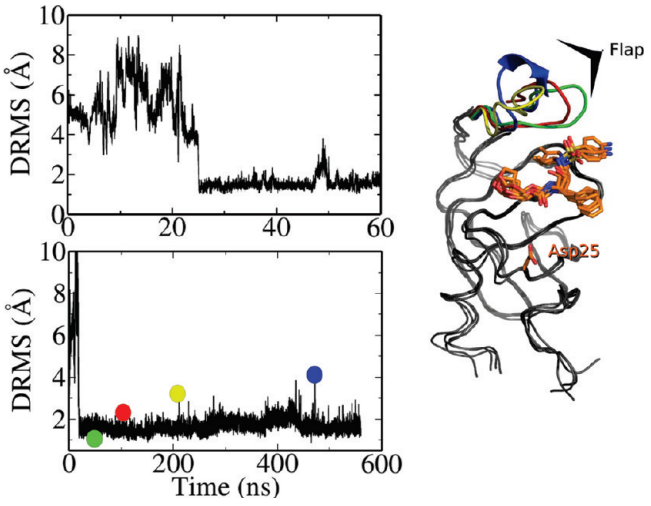

Figure 8. Spontaneous binding of DRV to monomeric HIV-1 PR and stability of the MD1 binding mode. (Left) Time series of DRMS from the MD1 binding mode for two of the eight runs that reached it spontaneously. The time series in the bottom refers to an elongated run and shows that the MD1 binding mode is stable over a time scale of 0.5 μs. Other time series of DRMS for the elongated runs are shown in Figure S10. (Right) Four MD snapshots extracted from one of the runs. DRV is shown by sticks with carbon atoms in orange, while monomeric HIV-1 PR is shown by a gray ribbon with the flap region in four different colors corresponding to the circles along the time series. Note that the MD1 binding mode is stable despite the motion at the flap and terminal segments.

DRV, while the dimerization of the V32I/L33I mutant is inhibited already at a DRV concentration of 0.1 μM.[9] The simulations show that DRV interacts with various positions of the monomeric HIV-1 PR surface. The frequencies of contact with more than 60 residues are higher than 30% for both mutants, which is likely due to the high concentration of DRV (15 mM) in the simulation box. Importantly, the contact frequencies comparison (Figure 4) shows that the largest differences between the two mutants are in the segments 45−57 and 79−83, which bracket the two residues that are different between these two mutants. In the MD1 binding mode (mutant V32I/L33I), there are favorable hydrophobic interactions between the side chains of Ile54 and the aniline ring of DRV as well as Val82 and the phenyl ring of DRV (Figure 6, bottom), which are less stable for the V32I/L33F/I54M/V82I mutant.

Finally, it was verified (by two simulations of 0.5 μs each) that the mutations in V32I/L33F/I54M/V82I do not prevent dimerization by a comparison of homodimeric HIV-1 PR wild type and the eight-point mutant V32I/L33F/I54M/V82I/V32′I/L33′F/I54′M/V82′I. The similar RMSD values and essentially identical RMSF profiles along the sequence (Figure S13) show that the structural stability and flexibility, respectively, are not influenced by the additional point mutations. Taken together, the simulation results obtained with monomeric and dimeric HIV-1 PR indicate that the resistance to DRV of the V32I/L33F/I54M/V82I variant is due to reduced binding of DRV to its monomeric structure rather than a lack of dimerization.

4. CONCLUSIONS

Among the many inhibitors of HIV-1 PR, 10 of which are in clinical use to treat AIDS, the drug DRV (Figure 1) is particularly interesting because its antiviral activity is not reduced by a large number of HIV-1 PR mutants, including clinical HIV strains isolated from AIDS patients. Inhibition of HIV-1 PR dimerization by DRV has been suggested as one of the reasons for the high genetic barrier against HIV's attainment of resistance to DRV,[9] but there is no direct experimental evidence of the binding of DRV to monomeric HIV-1 PR (e.g., a crystal structure of the complex). Moreover, the evidence for the stability of the monomeric fold is not definitive, as it is based on NMR spectroscopy data of mutants that destabilize the dimerization interface[14−16] and short MD simulations of the wild type.[10,11]

Here, multiple MD simulations of monomeric HIV-1 PR in the absence and presence of DRV were carried out to assess the structural stability of the monomer and identify the binding mode(s) of DRV, respectively. Three main results emerge from the analysis of a total of nearly 12 μs of explicit solvent MD sampling. First, excluding the flexible termini, the structure of monomeric HIV-1 PR is stable over a 0.1 μs time scale (12 MD runs without DRV) and is essentially identical to the one observed in the X-ray structure of the dimer. The RMSD of the 80 nonterminal Cα atoms is almost always smaller than 3.0 Å and smaller than 2.0 Å if one also excludes the 10 residues at the flap (Figure 3). The structural stability of monomeric HIV-1 PR (with bound DRV) is also observed over a 0.5 μs time scale in multiple MD simulations and with two different force fields.

Second, the MD simulations reveal a major binding mode to monomeric HIV-1 PR which is different from those in the crystal structure of the complex with mature HIV-1 PR. It is located at the substrate binding site and is mainly stabilized by the following hydrophobic interactions: the DRV isopropyl group with Ile32, Ile47, and Ile84; the DRV phenyl ring with Ile50 and Val82; the DRV aniline with Ile50, Ile54, Pro79, and Thr80; and the DRV bis-tetrahydrofuran group with Ala28, Ile32, Ile47, and Ile84 (Figure 6). The kinetic stability of this binding mode is further validated by five independent MD runs of 0.5 μs each during which the aforementioned intermolecular contacts are preserved (and the DRMS almost never exceeds 2.0 Å, Figure 8). Thus, the MD simulations show multiple stable interactions between DRV and several residues at the flap. These intermolecular interactions are likely to sterically interfere with the formation of the flap contacts which are present in the dimeric structure of the mature enzyme. Mutations at the flap residues Ile50 and Phe53 have been shown to affect the stability of the wild type dimer.[43] The MD simulation results and in particular the major binding mode suggest that interactions between DRV and the flap prevent the association of the flap of the other monomer (Figure 7) by a steric effect similar to the one of destabilizing mutations.

Third, two mutants V32I/L33I and V32I/L33F/I54M/V82I were investigated in detail because dimerization of the former is inhibited by DRV while the latter is not.[9] Multiple simulations starting from different initial positions and orientations of DRV show similar patterns of association to most of the HIV-1 PR surface. The largest differences in the contact maps are observed for residues 54 and 82, which bind DRV more in the case of monomeric V32I/L33I HIV-1 PR than for the V32I/L33F/I54M/V82I mutant (Figure 4). The less frequent binding of DRV to the mutant V32I/L33F/I54M/V82I is consistent with the reduced inhibition of dimerization measured by a FRET-based HIV-1 expression assay.[9]

Taken together, the stable binding mode to monomeric HIV-1 PR revealed by this MD study and experimental data, in particular the FRET measurements of inhibition of dimerization by DRV and kinetic binding studies, provide a possible explanation for the high genetic barrier and broad efficacy of DRV against HIV strains resistant to other HIV-1 PR inhibitors. The concentration of DRV in plasma is >4 μM in the patients treated by DRV and ritonavir, while in vivo concentration of HIV-1 PR is <50 nM.[8] Given the high concentration of DRV and low concentration of HIV-1 PR in plasma, a micromolar affinity of DRV for the monomer should be sufficient to significantly prevent the dimerization process. In addition, DRV has a conventional mechanism of inhibition of mature HIV-1 PR by strong binding to the active site. This mechanism plays the main role for the wild type because of the very high affinity of DRV for dimeric HIV-1 PR (dissociation constant smaller than 1 nM) and the very slow off-rate.[21] The dissociation constant of the homodimer/monomer equilibrium of wild type HIV-1 PR is about 10 nM, and binding of DRV further stabilizes the dimer[44] so that DRV does not disrupt mature HIV-1 PR. For some multidrug-resistant HIV-1 PR, a decrease in DRV binding affinity by a factor of about 1000 but full antiviral activity have been reported.[21] It is likely that for these clinical isolates not only the potency of DRV for the mature HIV-1 PR weakens but at the same time the dimer stability decreases. Thus, the main mechanism becomes less important, and the second mechanism, i.e., binding to the monomeric form of the protease and inhibition of dimerization, becomes dominant. With this dual mechanism, DRV antiviral activity does not change unless the mutations not only interfere with binding to the dimer but also to the monomer and/or lead to a more stable dimer. However, the chances for such mutants are significantly lower than in the case of a single mechanism of inhibition. Therefore, the dual mechanism of inhibition, i.e., binding to both dimer and monomer species, explains the superior resistance profile of DRV.

■ ASSOCIATED CONTENT

Supporting Information

PDB codes of 27 HIV-1 PR (mutants) complexed with DRV; figures of time series of RMSD for three independent runs of V32I/L33I, V32I/L33F/I54M/V82I, V32I/L33F/I54M/V82A, and V32I/L33F/I54M/I84V; radius of gyration; distances from the C atoms of residue Ile51 at the flap tip and residue Ile32 at the base of the active site; hydrophobic contacts; DRMS from the binding modes MD1 and MD2; DRMS from the binding mode MD1 with Amber force field; RMSD and RMSF for dimer protein; distance of protein atom to DRV; stability of DRV along the 0.5 μs simulations; and single-exponential kinetics of unbinding of DRV from the exterior surface of the flap. This material is available free of charge via the Internet at http://pubs.acs.org.

■ AUTHOR INFORMATION

Corresponding Author

*Phone: (+41 44) 635 55 21. Fax: (+41 44) 635 68 62. E-mail: dhuang@bioc.uzh.ch, caflisch@bioc.uzh.ch.

Notes

The authors declare no competing financial interest.

■ ACKNOWLEDGMENTS

We thank Dr. Alexander Bienz for useful discussions and Drs. Michele Seeber and Gianni Settanni for help with the program WORDOM. We also thank Drs. Yufeng Cai and Celia Schiffer for kindly providing the Amber force field parameters of Darunavir. The simulations were carried out on the Schrödinger cluster at the University of Zurich. This work was supported by a grant of the Swiss National Science Foundation to A.C.

■ REFERENCES

(1) Kohl, N. E.; Emini, E. A.; Schleif, W. A.; Davis, L. J.; Heimbach, J. C.; Dixon, R. A.; Scolnick, E. M.; Sigal, I. S. Active human immunodeficiency virus protease is required for viral infectivity. *Proc. Natl. Acad. Sci. U. S. A.* **1988**, *85*, 4686−4690.

(2) Rang, H. P.; Dale, M. M.; Ritter, J. M.; Flower, R. J. *Rang and Dale's Pharmacology*, 6th ed.; Churchill Livingstone Elsevier: Philadelphia, PA, 2007.

(3) Watkins, T.; Resch, W.; Irlbeck, D.; Swanstrom, R. Selection of high-level resistance to human immunodeficiency virus type 1 protease inhibitors. *Antimicrob. Agents Chemother.* **2003**, *47*, 759−769.

(4) Ferrer, E.; Podzamczer, D.; Arnedo, M.; Fumero, E.; McKenna, P.; Rinehart, A.; Prez, J. L.; Barber, M. J.; Pumarola, T.; Gatell, J. M.; Team, C. S. Genotype and phenotype at baseline and at failure in human immunodeficiency virus,infected antiretroviral-naive patients in a randomized trial comparing zidovudine and lamivudine plus nelfinavir or nevirapine. *J. Infect. Dis.* **2003**, *187*, 687−690.

(5) MacArthur, R. D. Darunavir: promising initial results. *Lancet* **2007**, *369*, 1143−1144.

(6) Ghosh, A. K.; Dawson, Z. L.; Mitsuya, H. Darunavir, a conceptually new HIV-1 protease inhibitor for the treatment of drug-resistant HIV. *Bioorg. Med. Chem.* **2007**, *15*, 7576−7580.

(7) Madruga, J. V.; Berger, D.; McMurchie, M.; Suter, F.; Banhegyi, D.; Ruxrungtham, K.; Norris, D.; Lefebvre, E.; de Bthune, M.-P.; Tomaka, F.; Pauw, M. D.; Vangeneugden, T.; Spinosa-Guzman, S. Efficacy and safety of darunavir-ritonavir compared with that of lopinavir-ritonavir at 48 weeks in treatment-experienced, HIV-infected patients in titan: a randomised controlled phase III trial. *Lancet* **2007**, *370*, 49−58.

(8) Koh, Y.; Matsumi, S.; Das, D.; Amano, M.; Davis, D.; Li, J.; Leschenko, S.; Baldridge, A.; Shioda, T.; Yarchoan, R.; et al. Potent inhibition of HIV-1 replication by novel non-peptidyl small molecule inhibitors of protease dimerization. *J. Biol. Chem.* **2007**, *282*, 28709.

(9) Koh, Y.; Aoki, M.; Danish, M.; Aoki-Ogata, H.; Amano, M.; Das, D.; Shafer, R.; Ghosh, A.; Mitsuya, H. Loss of protease dimerization inhibition activity of darunavir is associated with the acquisition of resistance to darunavir by HIV-1. *J. Virol.* **2011**, *85*, 10079−10089.

(10) Levy, Y.; Caflisch, A. Flexibility of monomeric and dimeric HIV-1 protease. *J. Phys. Chem. B* **2003**, *107*, 3068−3079.

(11) Levy, Y.; Caflisch, A.; Onuchic, J. N.; Wolynes, P. G. The folding and dimerization of HIV-1 protease: Evidence for a stable monomer from simulations. *J. Mol. Biol.* **2004**, *340*, 67−79.

(12) Broglia, R.; Levy, Y.; Tiana, G. HIV-1 protease folding and the design of drugs which do not create resistance. *Curr. Opin. Struct. Biol.* **2008**, *18*, 60−66.

(13) Bonomi, M.; Barducci, A.; Gervasio, F. L.; Parrinello, M. Multiple routes and milestones in the folding of HIV-1 protease monomer. *PLoS ONE* **2010**, *5*, e13208.

(14) Ishima, R.; Ghirlando, R.; Tözsér, J.; Gronenborn, A.; Torchia, D.; Louis, J. Folded monomer of HIV-1 protease. *J. Biol. Chem.* **2001**, *276*, 49110.

(15) Louis, J.; Ishima, R.; Nesheiwat, I.; Pannell, L.; Lynch, S.; Torchia, D.; Gronenborn, A. Revisiting monomeric HIV-1 protease. *J. Biol. Chem.* **2003**, *278*, 6085−6092.

(16) Ishima, R.; Torchia, D.; Lynch, S.; Gronenborn, A.; Louis, J. Solution structure of the mature HIV-1 protease monomer. *J. Biol. Chem.* **2003**, *278*, 43311−43319.

(17) Louis, J.; Ishima, R.; Aniana, A.; Sayer, J. Revealing the dimer dissociation and existence of a folded monomer of the mature HIV-2 protease. *Protein Sci.* **2009**, *18*, 2442−2453.
(18) Hartl, M.; Schweimer, K.; Reger, M.; Schwarzinger, S.; Bodem, J.; Rosch, P.; Wohrl, B. Formation of transient dimers by a retroviral protease. *Biochem. J.* **2010**, *427*, 197−203.
(19) Kovalevsky, A.; Liu, F.; Leshchenko, S.; Ghosh, A.; Louis, J.; Harrison, R.; Weber, I. Ultra-high resolution crystal structure of HIV-1 protease mutant reveals two binding sites for clinical inhibitor TMC114. *J. Mol. Biol.* **2006**, *363*, 161−173.
(20) Ghosh, A.; Dawson, Z.; Mitsuya, H. Darunavir, a conceptually new HIV-1 protease inhibitor for the treatment of drug-resistant HIV. *Bioorg. Med. Chem.* **2007**, *15*, 7576−7580.
(21) Dierynck, I.; De Wit, M.; Gustin, E.; Keuleers, I.; Vandersmissen, J.; Hallenberger, S.; Hertogs, K. Binding kinetics of darunavir to human immunodeficiency virus type 1 protease explain the potent antiviral activity and high genetic barrier. *J. Virol.* **2007**, *81*, 13845.
(22) Kovalevsky, A.; Ghosh, A.; Weber, I. Solution kinetics measurements suggest HIV-1 protease has two binding sites for darunavir and amprenavir. *J. Med. Chem.* **2008**, *51*, 6599−6603.
(23) Darke, P.; Jordan, S.; Hall, D.; Zugay, J.; Shafer, J.; Kuo, L. Dissociation and association of the HIV-1 protease dimer subunits: equilibria and rates. *Biochemistry* **1994**, *33*, 98−105.
(24) Berendsen, H.; van der Spoel, D.; Van Drunen, R. Gromacs: A message-passing parallel molecular dynamics implementation. *Comput. Phys. Commun.* **1995**, *91*, 43−56.
(25) Hess, B.; Kutzner, C.; Van Der Spoel, D.; Lindahl, E. Gromacs 4: Algorithms for highly efficient, load-balanced, and scalable molecular simulation. *J. Chem. Theory Comput.* **2008**, *4*, 435−447.
(26) MacKerell, A. D.; Bashford, D.; Bellott; Dunbrack, R. L.; Evanseck, J. D.; Field, M. J.; Fischer, S.; Gao, J.; Guo, H.; Ha, S.; Joseph-McCarthy, D.; Kuchnir, L.; Kuczera, K.; Lau, F. T. K.; Mattos, C.; Michnick, S.; Ngo, T.; Nguyen, D. T.; Prodhom, B.; Reiher, W. E.; Roux, B.; Schlenkrich, M.; Smith, J. C.; Stote, R.; Straub, J.; Watanabe, M.; Wirkiewicz-Kuczera, J.; Yin, D.; Karplus, M. All-atom empirical potential for molecular modeling and dynamics studies of proteins. *J. Phys. Chem. B* **1998**, *102*, 3586−3616.
(27) Jorgensen, W. L.; Chandrasekhar, J.; Madura, J.; Impey, R. W.; Klein, M. L. Comparison of simple potential functions for simulating liquid water. *J. Chem. Phys.* **1983**, *79*, 926−935.
(28) Vanommeslaeghe, K.; Hatcher, E.; Acharya, C.; Kundu, S.; Zhong, S.; Shim, J.; Darian, E.; Guvench, O.; Lopes, P.; Vorobyov, I.; Mackerell, A. D. J. CHARMM general force field: A force field for drug-like molecules compatible with the CHARMM all-atom additive biological force fields. *J. Comput. Chem.* **2010**, *31*, 671−690.
(29) Wang, J.; Wolf, R. M.; Caldwell, J. W.; Kollman, P. A.; Case, D. A. Development and testing of a general amber force field. *J. Comput. Chem.* **2004**, *25*, 1157−1174.
(30) Cai, Y.; Schiffer, C. A. Decomposing the energetic impact of drug resistant mutations in hiv-1 protease on binding drv. *J. Chem. Theory Comput.* **2010**, *6*, 1358−1368.
(31) Darden, T.; York, D.; Pedersen, L. G. Particle mesh Ewald: an Nlog(N) method for Ewald sums in large systems. *J. Chem. Phys.* **1993**, *98*, 10089.
(32) Bussi, G.; Donadio, D.; Parrinello, M. Canonical sampling through velocity rescaling. *J. Chem. Phys.* **2007**, *126*, 014101.
(33) Berendsen, H. J. C.; Postma, J. P. M; van Gunsteren, W. F.; DiNola, A.; Haak, J. R. Molecular dynamics with coupling to an external bath. *J. Chem. Phys.* **1984**, *81*, 3684−3690.
(34) Brooks, B. R.; Brooks, C. L., III; Mackerell, A. D. J.; Nilsson, L.; Petrella, R. J.; Roux, B.; Won, Y.; Archontis, G.; Bartels, C.; Boresch, S.; Caflisch, A.; Caves, L.; Cui, Q.; Dinner, A. R.; Feig, M.; Fischer, S.; Gao, J.; Hodoscek, M.; Im, W.; Kuczera, K.; Lazaridis, T.; Ma, J.; Ovchinnikov, V.; Paci, E.; Pastor, R. W.; Post, C. B.; Pu, J. Z.; Schaefer, M.; Tidor, B.; Venable, R. M.; Woodcock, H. L.; Wu, X.; Yang, W.; York, D. M.; Karplus, M. CHARMM: the biomolecular simulation program. *J. Comput. Chem.* **2009**, *30*, 1545−614.
(35) Seeber, M.; Cecchini, M.; Rao, F.; Settanni, G.; Caflisch, A. Wordom: a program for efficient analysis of molecular dynamics simulations. *Bioinformatics* **2007**, *23*, 2625.
(36) Seeber, M.; Felline, A.; Raimondi, F.; Muff, S.; Friedman, R.; Rao, F.; Caflisch, A.; Fanelli, F. Wordom: A user-friendly program for the analysis of molecular structures, trajectories, and free energy surfaces. *J. Comput. Chem.* **2011**, *32*, 1183−1194.
(37) Krivov, S.; Karplus, M. One-dimensional free-energy profiles of complex systems: Progress variables that preserve the barriers. *J. Phys. Chem. B* **2006**, *110*, 12689−12698.
(38) Krivov, S. V.; Muff, S.; Caflisch, A.; Karplus, M. One-dimensional barrier-preserving free-energy projections of a-sheet miniprotein: New insights into the folding process. *J. Phys. Chem. B* **2008**, *112*, 8701−8714.
(39) Freedberg, D.; Ishima, R.; Jacob, J.; Wang, Y.; Kustanovich, I.; Louis, J.; Torchia, D. Rapid structural fluctuations of the free HIV protease flaps in solution: relationship to crystal structures and comparison with predictions of dynamics calculations. *Protein Sci.* **2002**, *11*, 221−232.
(40) Ishima, R.; Freedberg, D.; Wang, Y.; Louis, J.; Torchia, D. Flap opening and dimer-interface flexibility in the free and inhibitor-bound HIV protease, and their implications for function. *Structure* **1999**, *7*, 1047−1055.
(41) Eyal, E.; Gerzon, S.; Potapov, V.; Edelman, M.; Sobolev, V. The limit of accuracy of protein modeling: influence of crystal packing on protein structure. *J. Mol. Biol.* **2005**, *351*, 431−442.
(42) Case, D. A.; Cheatham, T. E.; Darden, T.; Gohlke, H.; Luo, R.; Merz, K. M.; Onufriev, A.; Simmerling, C.; Wang, B.; Woods, R. J. The amber biomolecular simulation programs. *J. Comput. Chem.* **2005**, *26*, 1668−1688.
(43) Liu, F.; Kovalevsky, A.; Tie, Y.; Ghosh, A.; Harrison, R.; Weber, I. Effect of flap mutations on structure of HIV-1 protease and inhibition by saquinavir and darunavir. *J. Mol. Biol.* **2008**, *381*, 102−115.
(44) Sayer, J.; Liu, F.; Ishima, R.; Weber, I.; Louis, J. Effect of the active site D25N mutation on the structure, stability, and ligand binding of the mature HIV-1 protease. *J. Biol. Chem.* **2008**, *283*, 13459−13470.
(45) Wallace, A. C.; Laskowski, R. A.; Thornton, J. M. LIGPLOT: a program to generate schematic diagrams of protein-ligand interactions. *Protein Eng.* **1995**, *8*, 127−134.
(46) DeLano, W. L. *The PyMOL Molecular Graphics System*; DeLano Scientific: San Carlos, CA, 2002; http://www.pymol.org.